Lab on a Chip

PAPER

View Article Online
View Journal



Cite this: DOI: 10.1039/c4lc00716f

# Blood coagulation screening using a paper-based microfluidic lateral flow device†

H. Li,[a] D. Han,[a] G. M. Pauletti[b] and A. J. Steckl*[a]

Received 18th June 2014,
Accepted 13th August 2014

DOI: 10.1039/c4lc00716f

www.rsc.org/loc

A simple approach to the evaluation of blood coagulation using a microfluidic paper-based lateral flow assay (LFA) device for point-of-care (POC) and self-monitoring screening is reported. The device utilizes whole blood, without the need for prior separation of plasma from red blood cells (RBC). Experiments were performed using animal (rabbit) blood treated with trisodium citrate to prevent coagulation. $CaCl_2$ solutions of varying concentrations are added to citrated blood, producing $Ca^{2+}$ ions to re-establish the coagulation cascade and mimic different blood coagulation abilities *in vitro*. Blood samples are dispensed into a paper-based LFA device consisting of sample pad, analytical membrane and wicking pad. The porous nature of the cellulose membrane separates the aqueous plasma component from the large blood cells. Since the viscosity of blood changes with its coagulation ability, the distance RBCs travel in the membrane in a given time can be related to the blood clotting time. The distance of the RBC front is found to decrease linearly with increasing $CaCl_2$ concentration, with a travel rate decreasing from 3.25 mm $min^{-1}$ for no added $CaCl_2$ to 2.2 mm $min^{-1}$ for 500 mM solution. Compared to conventional plasma clotting analyzers, the LFA device is much simpler and it provides a significantly larger linear range of measurement. Using the red colour of RBCs as a visible marker, this approach can be utilized to produce a simple and clear indicator of whether the blood condition is within the appropriate range for the patient's condition.

## 1. Introduction

Cardiovascular disease is a leading cause of death worldwide.[1] Coagulation, the process by which blood forms clots, involves a cascade of interactions between blood platelets, proteins and various coagulation factors.[2] Physiologically, blood coagulation rapidly limits blood loss from a damaged vessel. For many patients, however, inhibition of blood coagulation using blood-thinning medication (anticoagulants), such as heparin or warfarin, is required to reduce the risk for stroke, pulmonary embolism, heart attack, and other life-threatening cardiovascular diseases. Constant monitoring of long-term anticoagulation efficacy is critical for these patients. If the anticoagulant drug level is too low, the risk of blood clot formation is high. Conversely, if the drug level is too high, severe bleeding (hemorrhage) can occur. Monitoring of anticoagulation therapy is usually performed by trained specialists in a hospital or laboratory setting.

To reduce the cost of care and to allow more frequent measurements, there is a strong impetus for the development of point-of-care (POC) and self-monitoring testing devices that can be used directly by patients or their caregivers.[3] In addition to patient convenience and rapid test results, frequent monitoring of anticoagulation efficacy reduces the risk of bleeding or thrombotic complications. Existing portable coagulation devices[4] are designed primarily for POC testing and use a variety of fairly complex methods of measurement, such as amperometric, electrochemical and photo-mechanical end-point detection. While this provides a high level of accuracy, it results in a product that is quite expensive ($1000–5000 range for the instrument and $1–10 per test strip) making them beyond the reach of a large segment of the population. Features of several commercial products available for portable POC and self-monitoring can be found in ref. 4. The aim of this work is to establish the feasibility of a blood coagulation self-monitoring approach that can provide a device that is orders of magnitude less expensive.

Microfluidics has been utilized to miniaturize analytical systems[5] in order to reduce sample volumes and analysis time and to increase versatility of procedures. Several blood-related applications of microfluidics have been reported for separation and analysis of cells and plasma. These applications have been reviewed by Toner and Irimia[6] and by Lim and colleagues.[7] A few representative examples include the

[a] Department of Electrical Engineering and Computing Systems, College of Engineering and Applied Science, University of Cincinnati, Cincinnati, OH, USA 45221. E-mail: a.steckl@uc.edu
[b] James L. Winkle College of Pharmacy, University of Cincinnati, Cincinnati, OH, USA 45221

† Electronic supplementary information (ESI) available. See DOI: 10.1039/c4lc00716f

separation of red and white blood cells from plasma using magnetic properties of cells,[8] the use of immunomagnetic beads to cleanse blood of pathogens,[9] the separation of plasma fibrinogen and the measurement of the plasma coagulation onset using lithographically formed micropillars.[10,11] These approaches have utilized relatively complex device structures fabricated on glass or plastic substrates.

For POC and self-monitoring applications, simplicity of the device is important both in terms of product cost and its operation. Conventional microfluidic devices utilize pressure driven flow for fluid transport, which is provided by syringe-type pumps and associated control units. This increases the complexity of the operation and the cost of the overall system. Approaches have been reported to simplify the operation of microfluidic blood analysis devices by providing a built-in driver for fluid transport by developing capillary force in bead-packed microchannels[12] or using pre-installed low pressure (vacuum) to drive the flow.[13]

Another approach in the quest for simplicity and ease of operation of POC devices is the use of capillary flow in cellulose membranes. Paper-based microfluidic lateral flow assays (LFA) POC products for pregnancy and viruses (among others) have been commercially available[14] for several decades. More recently, paper-based devices for various electronic applications have been shown[15,16] to be a very versatile approach with potentially low cost. Since the pioneering work[17] of the Whitesides group with the fabrication of very simple microfluidic devices on paper for rapid diagnostic tests, paper-based LFA devices have been developed[18–21] for screening a variety of conditions and situations: human and animal health and disease, environmental monitoring, food safety, *etc.* The low cost of the paper and other materials utilized in the diagnostic devices encourages broader and more frequent utilization, while their one-time use minimizes contamination risks. In addition to the potential low cost aspect, the paper diagnostic device concept has environmental benefits since paper is a renewable and biodegradable resource. Various sensing methods[22–26] and network geometry[27,28] of paper devices have been developed, giving paper-based microfluidics great potential for applications in quantitative and sequential assays.

In this manuscript, the use of paper-based LFA for detecting blood coagulation ability is presented. As shown in Fig. 1, whole blood is a very rich medium, which is made up of approximately 45% by volume cells – erythrocytes (red blood cells – RBC), leukocytes (white blood cells – WBC) and platelets. More than 99% of cells in blood are RBCs. The remaining 55% of whole blood is protein-rich plasma, consisting of mostly water, with dissolved proteins, gas and ions. After an injury, human blood outside the vascular system clots within 2–6 min, following a sequential process (coagulation cascade) that is highly regulated by various proteins (coagulation factors) and critically depends on free $Ca^{2+}$ ions. Addition of sodium citrate to fresh whole blood binds $Ca^{2+}$ ions and, hence, prevents coagulation.[29,30] In this study, non-coagulating citrated rabbit blood[31] is the starting point for experiments. By adding various amounts of free $Ca^{2+}$ ions into citrated blood, the coagulation process is initiated and investigated under controlled conditions, thus being able to mimic blood coagulation properties *in vitro*. Recently, the paper-based separation of plasma from blood by antibody induced RBC agglutination was reported.[32] This approach requires the pre-spotting on the paper device of several antibodies covering all main blood groups.

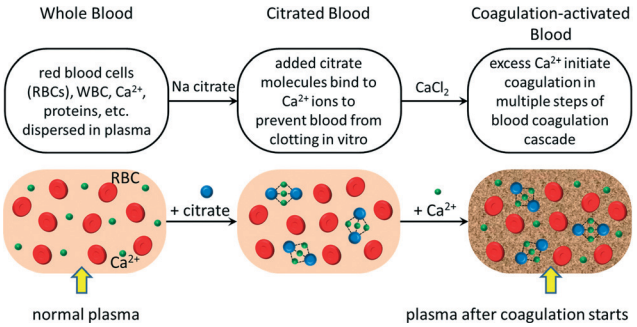


**Fig. 1** Simplified illustration of the nature of *in vivo* whole blood, commercially available anti-coagulated (citrated) whole blood, and coagulation-activated (by addition of $Ca^{2+}$) blood used for coagulation diagnostics on LFA devices.

## 2. Materials and methods

### 2.1 Materials and chemicals

Citrated rabbit whole blood (HemoStat Laboratories, Dixon, CA) was used as the substitute of human whole blood. According to the supplier, the volume ratio of rabbit whole blood to citrate solution [4% w/v trisodium citrate (Sigma-Aldrich) in water] is 4 to 1. This corresponds to a significant amount of citrate beyond what is needed for $Ca^{2+}$ immobilization.[31] Citrated rabbit plasma was obtained by centrifugation of the citrated rabbit whole blood (see sec. Fibrintimer samples). Various concentrations (50 mM to 500 mM; 50 mM increment) of $CaCl_2$ (Fisher Scientific) aqueous solutions were added to citrated rabbit whole blood as coagulants to mimic fresh human whole blood. 0.9 wt.% NaCl (Fisher Scientific) aqueous solution was used for blood sample dilution. 6 wt.% 2000 kDa dextran (Sigma-Aldrich) aqueous solution was used as a comparison to citrated rabbit blood when testing the unique effect of $Ca^{2+}$ ions.

Millipore HF075 nitrocellulose membrane was used as analytical membrane in the test strip on which blood coagulation took place. The HF075 membrane used in this study has a water flow rate of 0.5 mm $s^{-1}$, which is within the range specified[33] by the manufacturer [75 ± 19 s per 4 cm (0.71 mm $s^{-1}$ to 0.43 mm $s^{-1}$)]. The porosity of the various membranes in the LFA was measured using the water uptake method. The HF075 membrane has a porosity of 78.0%. Millipore G041 fiberglass membrane was used as sample pad due to its high porosity (~93%), through which plasma and blood cells can move easily. Millipore C048 cellulose paper, used as wicking pad to provide continuous capillary force, has a measured flow rate of 0.63 mm $s^{-1}$ and a porosity of 72.3%. The pore

size of nitrocellulose membranes used in LFAs ranges from 3–20 μm.[34] While the diameter of RBCs is typically in the 6–8 μm range,[6] they are highly deformable and are known[32,35,36] to pass through membranes with pore diameter as small as 2.5–3 μm.

### 2.2 LFA device

An LFA device was developed and utilized in the experiment. As shown in Fig. 2a, the test kit consists of a two-piece cassette that is designed to snap together. The top piece has a dispensing window that also serves as a reservoir to contain sample liquid and a second window opening to observe fluid flow transport. In the experiments the blood sample is dispensed into the reservoir and then is automatically transported to the test strip through capillary action. The test strip consists of four components – sample pad, analytical membrane, wicking pad and membrane backing. The strip is placed inside alignment ridges of the cassette, with the sample pad beneath the reservoir and the analytical membrane visible through the observation window, as shown in Fig. 2b. This provides good alignment between test strip and cassette, and good reproducibility of the LFA devices and experimental results.

During experiments, a blood sample was dispensed into the reservoir, absorbed by the sample pad, and then transported onto and through the analytical membrane. The cassette pieces are designed such that the wall of the dispensing reservoir is lightly pressed onto the sample pad when the cassette is snapped together. The blood sample soaks the sample pad and flows onto the analytical membrane in a controlled manner. As whole blood flows through the membrane, separation of RBCs from plasma occurs, with the plasma fraction moving much faster than the RBCs. This process is illustrated in the middle panel of Fig. 2, where the top piece of a LFA cassette is removed after a blood sample experiment is performed. In this particular experiment a small amount of whole blood was dispensed in order to show both the plasma and RBC fronts on the nitrocellulose membrane. In a typical 4 minute long experiment, the plasma reaches the wicking pad at an early stage of RBC transport, wetting the entire membrane and providing continuous capillary driving force during the measurement.

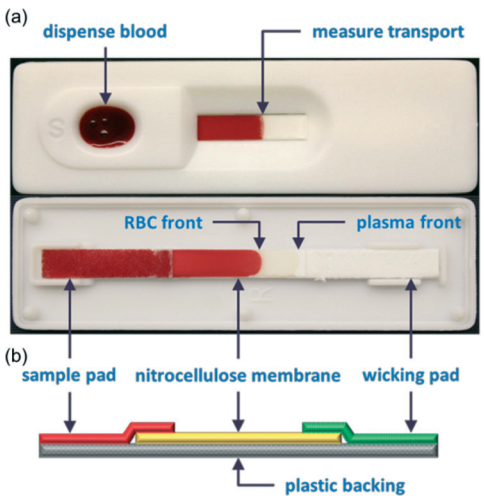


Fig. 2 Blood coagulation screening using lateral flow in paper-based devices: (a) photographs of an as-used assembled device (top) and of the device with the top piece removed to show the flow and device components; (b) schematic of the flow components.

### 2.3 Sample preparation

**LFA samples.** In LFA experiments, 160 μL of citrated rabbit blood was added to 5 μL 0.9% NaCl solution, followed by adding 15 μL $CaCl_2$ solutions (50 mM to 500 mM; increment 50 mM). For the control experiments without $CaCl_2$ addition, 15 μL 0.9% NaCl solution was used as a substitute for the 15 μL $CaCl_2$ solution to maintain blood cell concentration constant in sample fluid for all cases. All solutions were pre-heated to 39 °C. After each blood sample was made, it was incubated in the 39 °C water bath for an additional 2 min to initiate the blood coagulation process by providing an environment similar to rabbit's body. Immediately after the water bath, a volume of 100 μL from the overall sample was dispensed into the LFA inlet.

**Fibrintimer samples.** For comparison to LFA experiments, a CoaData 2000 Fibrintimer® (American LAbor, Durham, NC) was used to determine the clotting time of plasma obtained by centrifugation of citrated rabbit whole blood samples. The clotting time measurement started from the moment of adding coagulant ($CaCl_2$ solution) to the plasma and ended at the moment of detectable fibrin clot formation. The turbo-densitometric method utilized in the Fibrintimer® is a sensing method that combines stirring action and optical density measurement.

Plasma samples were obtained by centrifugation (Eppendorf MiniSpin, Germany) of citrated rabbit whole blood at 600× g for 10 min. A cuvette containing 80 μL of citrated rabbit plasma was placed into the reaction chamber first for incubation at 37 °C (fixed temperature in instrument). After 2 min, 100 μL of pre-mixed coagulation activating solution (15 μL $CaCl_2$ solution and 85 μL 0.9% NaCl solution) was added to the cuvette to initiate the coagulation process and the timer was started. $CaCl_2$ solution with several concentrations from 100 mM to 500 mM, in increments of 100 mM, has been used. A 250 mM $CaCl_2$ solution was also included.

## 3. Results and discussion

### 3.1 LFA measurements

The progress of RBCs in LFA devices is illustrated in the photographs of Fig. 3 as a function of added $CaCl_2$. The photographs were taken at 240 s after the moment when RBCs can be just visible in the device window for the first time. From the photographs it can be clearly observed that RBC travel distance (over a fixed time) decreases with increasing $CaCl_2$ concentration. This confirms that the introduction of $Ca^{2+}$ ions from the added $CaCl_2$ solution affects the blood

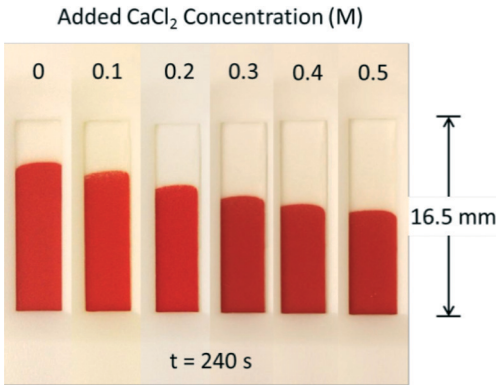


**Fig. 3** Photographs of LFA devices showing the transport of citrated whole blood at 240 s for several concentrations of added $CaCl_2$ solutions.

coagulation process in the LFA device and that the overall process has the potential to be used as a guide for blood coagulation screening and diagnosis.

Fig. 4 shows the relationship between the distance that blood samples travelled and their corresponding travel time through the nitrocellulose membrane in LFA device when $CaCl_2$ solutions with various concentrations (0 to 500 mM) were added. In Fig. 4, the (travel distance)$^2$ *vs.* time for the plasma and RBC fronts are plotted on a linear scale. The plasma component travels much faster than the RBCs, reaching the end of the observation window (coincident with the edge of the wicking pad) in 90 s (for low or no added $Ca^{2+}$ concentrations) to 120 s (for high added $Ca^{2+}$ concentration). As expected, the RBC flow rate is significantly slower and more strongly affected by the addition of $Ca^{2+}$ ions. The RBC front does not reach the wicking pad in any of the samples, even in the absence of added $Ca^{2+}$ ions. It is apparent that both blood components follow fairly closely the Washburn equation,[37] $L^2 = \gamma Dt/4\eta$, where $L$ is the travel distance, $\gamma$ is the surface tension, $D$ is the effective pore diameter, $t$ is the travel time and $\eta$ is the viscosity. The reduction in the slope of the measured travel distance with time for samples with increasing $CaCl_2$ concentration is related to the time

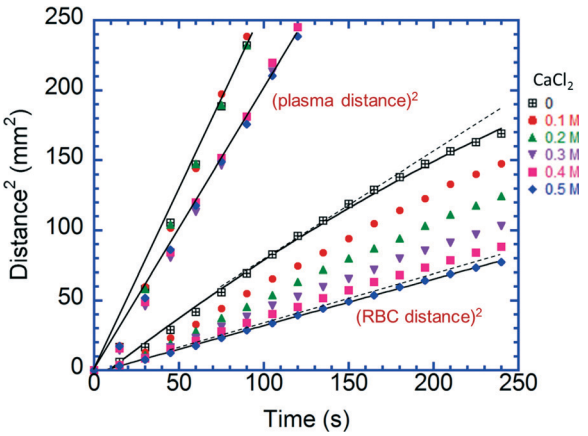


**Fig. 4** Transport of RBCs and plasma in LFA devices: (travel distance)$^2$ *vs.* time for RBCs and plasma components of whole blood samples.

derivative of the Washburn equation, which is proportional to the ratio of the surface tension to viscosity. As the added $Ca^{2+}$ ion concentration increases, the resulting enhancement in the coagulation process increases the effective viscosity of both plasma and RBC components of the blood sample. The deviation from agreement with pure Washburn flow (shown by the dashed lines) starts at a flow time of ~120–130 s and is most pronounced for samples where the RBC flow distance is the longest, namely the sample with no $CaCl_2$ added. Since we are dealing with a limited fluid volume, this effect is probably due to the evaporation of the plasma that occurs for longer times and distances, which in turn affect the capillary force present.

It is important to point out that for plasma transport in whole blood samples with different concentrations of added $CaCl_2$, the effect of $Ca^{2+}$ ions on plasma flow is fairly small. Unlike what is observed from RBC transport, plasma flow rate does not decrease significantly when more $Ca^{2+}$ ions are added. This demonstrates that RBCs are necessary to visualize the coagulation process in the plasma during which fibrin threads are gradually formed throughout the membrane, thus significantly slowing down the movement of RBCs.

As discussed above, the travel time of biological fluids in LFA devices is strongly affected by their viscosity. Once the relationship between the viscosity and the travel time of liquids is established in a particular LFA device, one can determine the viscosity of sample fluids based on their travel time in the LFA. To accomplish this in the case of blood plasma, solutions of glycerin and water have been utilized. Glycerin–water mixtures with up to 65 wt.% glycerin have an increase in viscosity of up to ~15× compared to plain water (~1 cP), while their surface tension exhibits only a negligible variation (~5%). Travel times of mixtures were measured until the liquid front reached a distance of 16.5 mm from the starting location. The travel times of several glycerin–water mixtures (from 0 to 65 wt.%) and their corresponding viscosities are shown in Fig. 5 (blue dots). Interestingly, these results provide a linear relationship between LFA travel time and the viscosity of the liquid. Furthermore, the slope of the linear relationship can be adjusted by selecting nitrocellulose membranes of different lengths or flow speeds. For example, denser membranes (*e.g.* HF240) with slower flow rate than HF075 will result in a larger time change with viscosity, thus providing higher resolution in the low viscosity range. Most importantly, these results demonstrate that LFA devices can provide sufficient resolution to detect a small variation of blood/plasma viscosity, such as those found in certain medical conditions. Based on the linear relationship developed for glycerine–water mixtures, the viscosities of plasma with different $CaCl_2$ concentrations can be obtained using their respective LFA travel time. The effective viscosity values calculated for plasma separated from the whole blood within LFA devices are ~5.0 cP for the case of no added $CaCl_2$ and ~5.8 cP when 500 mM $CaCl_2$ was added. The viscosity value calculated for pure plasma on LFA devices (obtained by centrifugation)

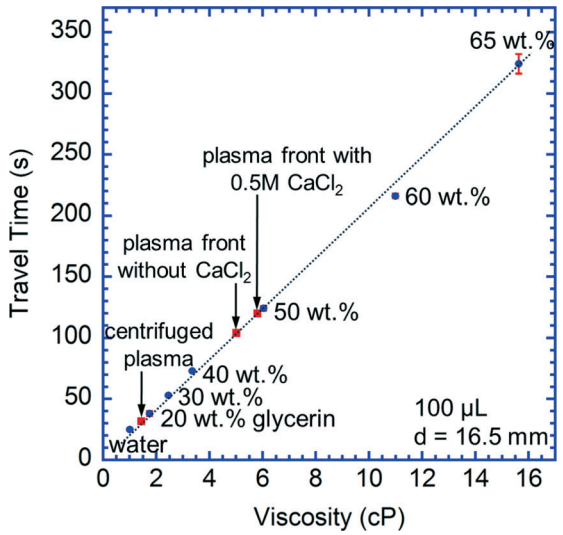


**Fig. 5** LFA travel time of glycerin/water samples (blue circles) with similar surface tension *vs.* their viscosity. Travel time of several plasma samples (red squares) indicates their effective viscosity. Nitrocellulose strip length – 16.5 mm.

is significantly lower (~1.4 cP) because there is no interaction with blood cells.

To verify the exclusive effect of $Ca^{2+}$ ions on citrated blood transport, similar experiments were conducted with dextran samples to which $CaCl_2$ solutions were added. Dextran is a polysaccharide that is used in solution to act as a replacement for blood plasma in cases of severe blood loss. The dextran solution utilized in these experiments has a viscosity of ~7.7 cP (measured using a falling-ball viscometer), which is in the range of anti-coagulated rabbit blood.[38] Except for using dextran solution instead of citrated blood, the other experimental conditions remained the same. Fig. 6a contains 3 sets of data from whole blood transport experiments in LFA devices as a function of added $CaCl_2$ concentration for a duration of 240 s. Companion dextran based experiments are included for comparison. A linear decrease in the normalized RBC travel distance with increasing $CaCl_2$ solution concentration is observed, which is consistent with Fig. 3. Agreements with ideal linearity for the three sets of data are 0.9782, 0.98461 and 0.98401, indicating good reproducibility of the experiments. Fig. 6a also clearly shows that the travel distance of the dextran solution is independent of the $CaCl_2$ additive. This demonstrates that $Ca^{2+}$ ions only alter the viscosity of the blood samples and not that of substitute fluids. Data range bars are introduced in this figure to cover all three values of the repeated sets of experiments for both citrated rabbit blood and dextran solution.

Fig. 6b compares the LFA travel of plasma *vs.* RBCs for travel times of 90 and 240 s. The plasma travel distance after 90 s for samples with added $CaCl_2$ solution concentrations from 0 to 500 mM is essentially constant, with only a slight decrease in distance between 200 and 300 mM. By contrast, RBC transport distance at both 90 and 240 s shows a monotonic decrease with increasing $CaCl_2$ concentration.

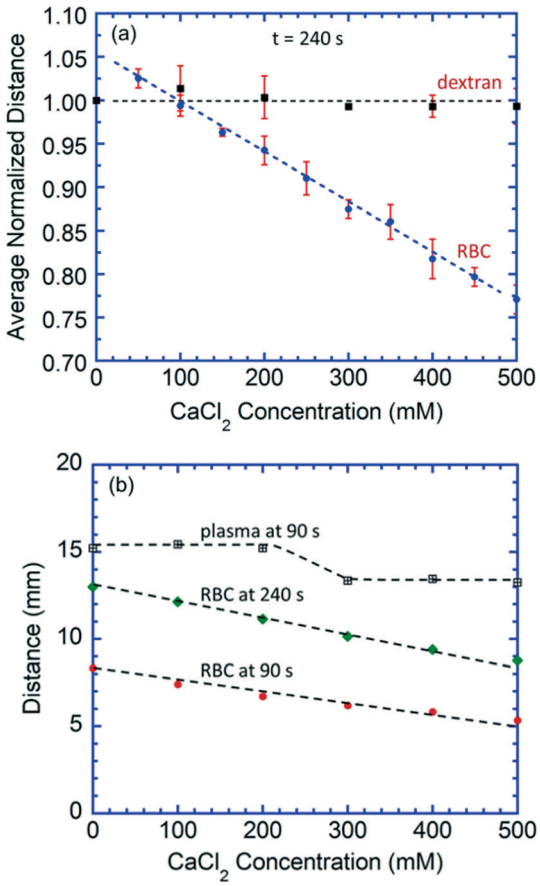


**Fig. 6** Travel distance in LFA as a function of $CaCl_2$ concentration: (a) normalized distance at 240 s for RBCs in whole blood samples and for dextran solutions; (b) travel of RBCs at 90 s and 240 s and of plasma (in whole blood) at 90 s.

The straight-line slope indicates that the RBC transport characteristics can eventually provide a quantitative, as well as qualitative, method of blood coagulation analysis.

### 3.2 Clotting time measurements

Measurements of clotting time in plasma samples centrifuged from citrated whole blood were performed using the CoaData 2000 Fibrintimer®. Fig. 7 shows the plasma clotting time as a function of $CaCl_2$ solution concentration. Experiments were performed 3 times to confirm reproducibility. No fibrin clot formation is detected when 100 mM $CaCl_2$ solution is added, which is probably due to insufficient amount of $Ca^{2+}$ ions to form a fibrin clot. As shown in Fig. 7, the clotting time decreases monotonically from ~1000 s for a $CaCl_2$ solution concentration of 200 mM to a minimum level of ~350 s for $CaCl_2$ solution concentration of 400–500 mM. The inset in Fig. 7 shows the relationship between the inverse of clotting time and the added $CaCl_2$ concentration. The relationship is linear for low $CaCl_2$ concentration up to 300 mM, and gradually reaches a plateau at ~400 mM. It is interesting to point out the similarity between the clotting time of citrated rabbit plasma as a function of $CaCl_2$ solution concentration shown

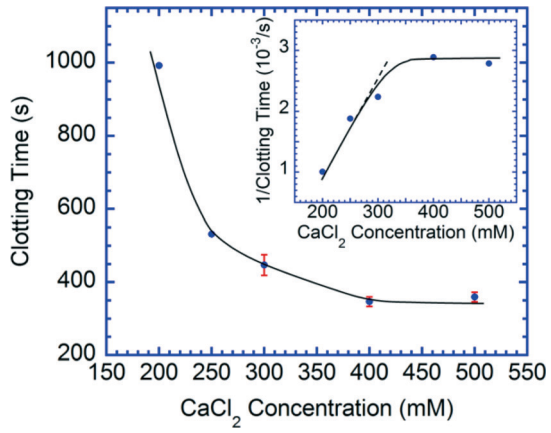


**Fig. 7** Plasma clotting time *vs.* $CaCl_2$ concentration measured using a CoaData 2000 Fibrintimer®. Inset: inverse of clotting time *vs.* $CaCl_2$ concentration.

in Fig. 7 and corresponding results reported[29] for the clotting time of citrated human plasma *vs.* free $Ca^{2+}$ ions within the plasma.

It is instructive to compare the results obtained with RBC transport in the LFA devices and plasma clotting results obtained with the CoaData 2000 Fibrintimer®. Fig. 8 contains the RBC travel distance in LFA devices and the plasma clotting times as a function of the concentration of added $CaCl_2$ solutions. For ease of comparison, three regions have been identified in the graph contained in Fig. 8. The RBC travel time is fixed at 240 s for all samples and the Fibrintimer® has a maximum detectable clotting time of 1000 s (~16 min).

Region 1 covers the addition of relatively low $CaCl_2$ concentration solutions, from none to 250 mM. At these low concentrations a relatively small number of $Ca^{2+}$ ions is added into the blood and plasma samples, therefore the coagulation effect is relatively weak. The plasma clotting time exceeds the Fibrintimer® limit until a 200 mM $CaCl_2$ solution is used, after which a sharp decrease in clotting time at 250 mM is observed. On the other hand, the RBC travel distance on LFA

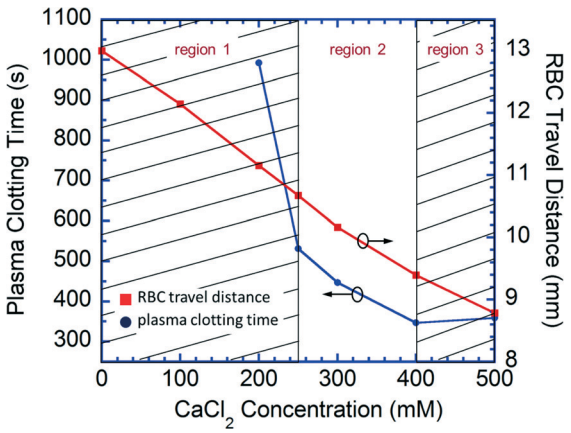


**Fig. 8** Comparison between data obtained from RBC travel distance (for 240 s) in LFA device and plasma clotting times obtained with CoaData 2000 Fibrintimer® as a function of $CaCl_2$ concentration.

devices displays a straight-line decrease with $CaCl_2$ concentration over the 0 to 250 mM range. Unlike plasma clotting measurements that only detect the effective end point of the coagulation process and which can be quite lengthy in the case of low/very low $Ca^{2+}$ ion concentration exceeding the time limit of available instruments, LFA-based measurements experience the whole blood coagulation process on the test strip in a matter of ~100–200 s. This makes the LFA device more sensitive to slight changes in coagulation ability that can be difficult to detect using the plasma clotting method. In region 2, both plasma clotting time and the RBC travel time display a straight-line decrease with increasing $CaCl_2$ solution concentration. Detection abilities of both approaches appear comparable in region 2. Finally, in region 3 that covers higher $CaCl_2$ solution concentrations (400–500 mM), while the measured clotting time becomes more or less constant at a value of ~350 s, the LFA device continues to provide a straight-line relationship. It is clear that the LFA approach provides a wider detection range with a linear response for coagulation diagnosis than that of conventional plasma clotting measurements.

## Summary and conclusions

In summary, a paper-based LFA approach for blood coagulation screening has been demonstrated. This very simple device has been shown to display a wide sensitivity range to $Ca^{2+}$ concentration (from a few mM to 500 mM) potentially superior to existing commercial clinical devices. Combined with their potentially low cost, this could result in the broad use of these LFA devices for diagnostic evaluation of individuals with both minor and acute coagulation conditions. The attractive cost and performance characteristics are of great advantage in drug monitoring activities, enabling single use of individual LFAs. Combined with disposal by incineration, this greatly minimizes any risk of contamination with bloodborne pathogens.

However, in order to make this approach a commercial reality several aspects will need to be pursued. This includes reducing the blood sample volume to levels similar to droplets typically withdrawn with finger-stick lancets (10–20 μL), determining reproducibility ranges and limiting factors, optimizing the materials in the LFA stack and the design of the cassette, and, of course, carrying out clinical trials that would validate the results for human subjects.

## Acknowledgements

This work was partially supported by the Bill and Melinda Foundation (grant # OPP1087022) and the National Science Foundation (ENG 1236987).

## Notes and references

1 *Promoting Cardiovascular Health in the Developing World: A Critical Challenge to Achieve Global Health*, ed. V. Fuster and B. B. Kelly, The National Academies Press, Washington D.C., 1st edn, 2010, ch. 2, pp. 49–50.

 

2 D. U. Silverthorn and B. R. Johnson, in *Human Physiology: An Integrated Approach*, Pearson/Benjamin Cummings, San Francisco, 6th edn, 2010, ch. 16, pp. 547–556.
3 J. A. Koepke, *Lab. Med.*, 2000, **31**, 343–346.
4 *Coagulation Analyzers – Point of Care, Self-Monitoring*, CAP Today, May 2011, pp. 28–36.
5 P. Tabeling, in *Introduction to Microfluidics*, Oxford University Press, Oxford, 1st edn, 2005, pp. 1–14.
6 M. Toner and D. Irimia, *Annu. Rev. Biomed. Eng.*, 2005, **7**, 77–103.
7 H. W. Hou, A. A. S. Bhagat, W. C. Lee, S. Huang, J. Han and C. T. Lim, *Micromachines*, 2011, **2**, 319–343.
8 K.-H. Han and A. B. Frazier, *Lab Chip*, 2006, **6**, 265–273.
9 C. W. Yung, J. Fiering, A. J. Mueller and D. E. Ingber, *Lab Chip*, 2009, **9**, 1171–1177.
10 M. M. Dudek, T. L. Lindahl and A. J. Killard, *Anal. Chem.*, 2010, **82**, 2029–2035.
11 M. M. Dudek, N. J. Kent, P. Gu, Z. H. Fan and A. J. Killard, *Analyst*, 2011, **136**, 1816–1825.
12 J. Shim, A. Browne and C. Ahn, *Biomed. Microdevices*, 2010, **12**, 949–957.
13 I. K. Dimov, L. Basabe-Desmonts, J. L. Garcia-Cordero, B. M. Ross, A. J. Ricco and L. P. Lee, *Lab Chip*, 2011, **11**, 845–850.
14 B. O'Farell, in *Lateral Flow Immunoassay*, ed. R. C. Wong and H. Y. Tse, Humana Press, New York, 1st edn, 2009, ch. 1, pp. 1–7.
15 D. Tobjörk and R. Österbacka, *Adv. Mater.*, 2011, **23**, 1935–1961.
16 A. Steckl, *IEEE Spectrum*, 2013, 48–61.
17 A. W. Martinez, S. T. Phillips, M. J. Butte and G. M. Whitesides, *Angew. Chem., Int. Ed.*, 2007, **46**, 1318–1320.
18 V. Gubala, L. F. Harris, A. J. Ricco, M. X. Tan and D. E. Williams, *Anal. Chem.*, 2011, **84**, 487–515.
19 A. K. Yetisen, M. S. Akram and C. R. Lowe, *Lab Chip*, 2013, **13**, 2210–2251.
20 X. Li, J. Tian and W. Shen, *Cellulose*, 2010, **17**, 649–659.
21 C. Parolo and A. Merkoci, *Chem. Soc. Rev.*, 2013, **42**, 450–457.
22 E. Carrilho, A. W. Martinez and G. M. Whitesides, *Anal. Chem.*, 2009, **81**, 7091–7095.
23 J. L. Delaney, C. F. Hogan, J. Tian and W. Shen, *Anal. Chem.*, 2011, **83**, 1300–1306.
24 A. K. Ellerbee, S. T. Phillips, A. C. Siegel, K. A. Mirica, A. W. Martinez, P. Striehl, N. Jain, M. Prentiss and G. M. Whitesides, *Anal. Chem.*, 2009, **81**, 8447–8452.
25 X. Liu, M. Mwangi, X. Li, M. O'Brien and G. M. Whitesides, *Lab Chip*, 2011, **11**, 2189–2196.
26 Z. Nie, C. A. Nijhuis, J. Gong, X. Chen, A. Kumachev, A. W. Martinez, M. Narovlyansky and G. M. Whitesides, *Lab Chip*, 2010, **10**, 477–483.
27 E. Fu, B. Lutz, P. Kauffman and P. Yager, *Lab Chip*, 2010, **10**, 918–920.
28 H. Liu and R. M. Crooks, *J. Am. Chem. Soc.*, 2011, **133**, 17564–17566.
29 F. I. Ataullakhanov, A. V. Pohilko, E. I. Sinauridze and R. I. Volkova, *Thromb. Res.*, 1994, **75**, 383–394.
30 E. P. Brass, W. B. Forman, R. V. Edwards and O. Lindan, *Blood*, 1978, **52**, 654–658.
31 D. G. Bjoraker and T. R. Ketcham, *Thromb. Res.*, 1981, **24**, 505–508.
32 X. Yang, O. Forouzan, T. P. Brown and S. S. Shevkoplyas, *Lab Chip*, 2012, **12**, 274–280.
33 *Millipore Hi-Flow™ Plus Membranes and SureWick® Pad Materials*, 2013.
34 M. A. Mansfield, in *Drugs of Abuse: Body Fluid Testing*, ed. R. C. Wong and H. Y. Tse, Humana Press, New York, 1st edn, 2005, ch. 4, p. 71.
35 R. Kowluru, M. W. Bitensky, A. Kowluru, M. Dembo, P. A. Keaton and T. Buican, *Proc. Natl. Acad. Sci. U. S. A.*, 1989, **86**, 3327–3331.
36 D. J. Beebe, G. A. Mensing and G. M. Walker, *Annu. Rev. Biomed. Eng.*, 2002, **4**, 261–286.
37 E. W. Washburn, *Phys. Rev.*, 1921, **17**, 273–283.
38 H.-G. Grigoleit, *Acta Diabetol. Lat.*, 1975, **12**, 72–78.